SAND98-0065C

SAND--98-0065C

Modeling Decomposition of Rigid Polyurethane Foam

Author: Michael L. Hobbs, Sandia National Laboratories

Address: Energetic and Multiphase Processes
Dept. 9112, MS 0834
Sandia National Laboratories
Albuquerque, NM 87185-0834

CONF-980804--

Phone: (505) 844-5988

FAX: (505) 844-8251

EMAIL: mlhobbs@sandia.gov

RECEIVED
JAN 29 1998
OSTI

Word Count: 5342

Word Count Calculation:

Abstract:	244
Text:	3532 (does not include abstract)
10 equations:	210
6 figures:	1200
2 tables:	400
Total:	5342

DISTRIBUTION OF THIS DOCUMENT IS UNLIMITED

MASTER

DISCLAIMER

Modeling Decomposition of Rigid Polyurethane Foam

Michael L. Hobbs*
Engineering Sciences Center, 9100
Sandia National Laboratories,
Albuquerque, New Mexico 87185

ABSTRACT

Rigid polyurethane foams are used as encapsulants to isolate and support thermally sensitive components within weapon systems. When exposed to abnormal thermal environments, such as fire, the polyurethane foam decomposes to form products having a wide distribution of molecular weights and can dominate the overall thermal response of the system. Decomposing foams have either been ignored by assuming the foam is not present, or have been empirically modeled by changing physical properties, such as thermal conductivity or emissivity, based on a prescribed decomposition temperature. The hypothesis addressed in the current work is that improved predictions of polyurethane foam degradation can be realized by using a more fundamental decomposition model based on chemical structure and vapor-liquid equilibrium, rather than merely fitting the data by changing physical properties at a prescribed decomposition temperature. The polyurethane decomposition model is founded on bond breaking of the primary polymer and formation of a secondary polymer which subsequently decomposes at high temperature. The bond breaking scheme is resolved using percolation theory to describe evolving polymer fragments. The polymer fragments vaporize according to individual vapor pressures. Kinetic parameters for the model were obtained from Thermal Gravimetric Analysis (TGA) from a single nonisothermal experiment with a heating rate of 20 C/min. Model predictions compare reasonably well with a separate nonisothermal TGA weight loss experiment with a heating rate of 200 C/min.

---

* This work performed at Sandia National Laboratories. Sandia is a multiprogram laboratory operated by Sandia Corporation, a Lockheed Martin Company, for the U.S. Department of Energy under contract DE-ACO4-94AL85000

INTRODUCTION

In certain weapon systems, components are isolated by rigid polyurethane foam. When exposed to an abnormal thermal environment, such as fire, various encapsulated components are designed to fail sequentially. Computational schemes used in hazards analysis are designed to accommodate mass loss associated with foam decomposition. For example, Fig 1 shows a calculation of a system consisting of a block of material containing nonreactive components exposed to a constant flux [1]. In this calculation, the encapsulating material was assumed to decompose based on temperature, without using a realistic decomposition mechanism. When exposed to abnormal thermal environments, such as fire, the polyurethane foam decomposes to form products having a wide distribution of molecular weights and can dominate the overall thermal response of the system.

Several groups studying the decomposition of large macromolecules have employed statistical network fragmentation models. For example, Solomon and coworkers [2] have implemented a computationally intensive Monte Carlo technique to describe the breakup of coal. Fletcher et al. [3-5] have used pseudo lattice structures referred to as Bethe lattices to obtain closed form solutions of the network statistics as derived by Fisher and Essam [6]. These closed form solutions parallel the determination of molecular weight distributions during polymer synthesis leading to the critical condition required to form infinite polymer networks referred to as “gels” by Flory [7].

The PolyUrethane Foam (PUF) decomposition model discussed in the present paper is based on three fundamental aspects of thermal decomposition: 1) a kinetic bond breaking mechanism, 2) lattice statistics to describe the evolving polymer fragments, and 3) vaporization of the small polymer fragments (oligomers) with high vapor pressures as discussed by Fletcher et al. [3-5]. A review of various decomposition models is given in [8]. The PUF model parameters include the Arrhenius kinetics controlling bond breaking, the initial bond population, the coordination number, and the average site molecular weight. The initial bond population is assumed to be composed of both strong bonds and weak bonds. The coordination number describes the connectivity of thermally stable sites by bonds.

CHEMICAL STRUCTURE

Detailed information regarding the chemical structure of the polyurethane foam is required to predict foam decomposition. For complex macromolecular structures, such as coal, chemical structure information has been obtained using solid-state NMR [9]. Structural units for *synthesized* macromolecules, such as polyurethane foams, can be inferred from the preparation techniques and ingredients used to make up the foam. Figure 2 shows a simplified synthesis of a polyurethane network. The analogous Bethe lattice, with the same average coordination number, is shown in Fig 3. Any two sites within the Bethe lattices are connected by only one path of bonds and sites. The advantages of using Bethe lattice approximations with percolation theory are discussed by Grant et al. [3]. Finite polymer fragments or oligomers are created as chemical bonds break at elevated temperatures. These finite fragments as well as the remaining network are shown in Fig 3 as thermally degraded foam.

The average bulk density of the polyurethane foam used in the present study is 400 kg/m^3 (25 lb/ft^3). The most common chemical structural units of the rigid polyurethane foam and the distribution of these structural units are shown in Fig 4 as estimated by Saunders [10] using manufacturing details and assuming equal reactivity of the hydroxyl groups. Various graphic representations of specific chemical structural units are also shown in Fig 4. These structural units have been assembled to give a representative picture of the foam. The model foam shows the polyurethane structure as a large matrix (essentially infinite) of toluene diisocyanate groups connected by aliphatic bridges made from trimethylol propane, adipic acid, diethylene glycol, and small amounts of phthalic anhydride.

As the bonds break at elevated temperatures, fragments of finite molecular weight are generated. The fragments, with low molecular weight and cooresponding high vapor pressures, evaporate as shown at the bottom of Fig 4. Higher molecular weight fragments, with low vapor pressures, remain in the condensed phase.

KINETIC MECHANISM

The kinetic scheme along with a graphical description is shown in Fig 5. This 9 step mechanism with 11 species describes four events: 1) competition between local crosslinking and side-chain formation within the primary polymer, 2) competition between side-chain evolution from the primary polymer and the formation of a secondary polymer, 3) competition between local crosslinking in the secondary polymer and side-chain formation within the secondary polymer, and 4) side-chain evolution from the secondary polymer.

The $\mathcal{L}$, L, δ, d, c_1, c_2, g_1, g_2, g_3, g_4, and g_5, represent labile bridge in the primary polymer, labile bridge in the secondary polymer, side-chains or "danglers" in the primary polymer, side-chains or "danglers" in the secondary polymer, stable or "charred" bonds in the primary polymer, stable or "charred" bonds in the secondary polymer, gas species 1, and gas species 2, etc., respectively. This nomenclature closely follows Grant et al. [3-5]. Reversible reactions are included to allow the "danglers" to reattach to the polymer. Such reactions will likely be more significant when the foam is degraded under confinement.

The reaction sequence begins when a weak bond, e.g. the ether bond of the ester group, is broken to form either a toluene diisocyanate (TDI) side-chain (δ in Fig 5) or evolves as a gas (g_1 in Fig 5) with concurrent stabilization of adjacent clusters forming a stable bond (c_1 in Fig 5). The TDI side-chains, referred to as danglers, may eventually evolve as light gas fragments (g_2 in Fig 5) through subsequent, slower reactions. A secondary polymer may evolve as two TDI side-chains react to form a weak bridge (L) with the subsequent evolution of CO_2 denoted as g_3. The molecular weight of L is twice the molecular weight of $\mathcal{L}$ minus the molecular weight of g_3. The degradation of the secondary polymer is assumed to be similar to the degradation of the primary polymer except the labile bridge has a higher molecular weight.

The proposed mechanism in Fig 5 is consistent with experimental observation. For Example, Erickson [11] has examined decomposition gases from decomposing polyurethane foam using TGA-FTIR analysis and has observed an increase in the ~N-C=O stretch region of the IR spectra (wave number of 2250) from evolving gases sampled at 350 C, 400 C, and 450 C.

Table 1 gives the mechanism, rate equations, and boundary conditions for the PUF model. The general reaction rate, r_j, for the PUF model bond breaking scheme is described by:

$$r_j = k_j(T) \prod_{i=1}^{11} N_i^{\mu_{ij}} \quad , \qquad j = 1, \ldots 9 \tag{1}$$

where N_i represents either bond population parameters $\mathcal{L}$, L, δ, d, c_1, and c_2 or species parameters g_1, g_2, g_3, g_4, g_5. The concentration matrix is represented by μ_{ij} is ~~also~~ as given in Table 1. The expressions for the kinetic coefficients, $k_j(T)$, are given in an Arrhenius form:

$$k_j(T) = A_j exp(-E_j/RT) \tag{2}$$

where A_j (1/s), E_j (cal/mol or J/mol), and R (1.987 cal/mol-K or 8.314 J/mol-K) are the pre-exponential factors, activation energies, and the universal gas constant, respectively. The species rate of change is given by:

$$dN_i/dt = \sum_{j=1}^{J} \nu_{ij} r_j \quad , \qquad i = 1, \ldots I \tag{3}$$

where ν_{ij} are the stoichiometric coefficients of the jth reaction as given in Table 1. The kinetic mechanism requires the Arrhenius parameters A_j, and E_j to be supplied for each reaction. The initial labile bridge population ($\mathcal{L}_0$) and the initial strong bond population (c_0) need to be specified as an initial condition. These parameters may represent the extent of polymer curing. The initial value problem described by Eq. (1)-(3) is solved using DEBDF [12], a variable order backward difference ordinary differential equation solver package.

STATISTICAL MODEL

The Bethe lattice statistical model is referred to as *percolation theory* since the technique has been used historically to described fluid flow through a network of permeable and impermeable sites. Percolation theory is used to characterize the degraded foam structure with regard to the size and concentration of finite fragments or oligomers. The size and population of oligomers is based on the population of intact bonds, p, determined as follows:

$$p = \mathcal{L} + \mathrm{L} + c_1 + c_2 . \tag{4}$$

Percolation theory is computationally fast, reproducible, and replicates results from more versatile, yet computationally demanding, Monte Carlo methods [13]. Monte Carlo techniques generate random numbers between 0 and 1 for each bond. The bonds are either intact (if the random number is between 0 and p) or broken (if the random number is between p and 1). Monte Carlo techniques can be used with realistic chemical structures provided large realizations with many bonds are used to describe the large macromolecules.

One advantage of the Monte Carlo technique over percolation theory is that the polymer fragments can be removed from the network and quenched without affecting the decomposition kinetics of the parent foam structure. If the gas-phase polymer fragments, referred to as oligomers in the present paper, are kept at the same temperature as the parent foam, the oligomers thermally crack to form lighter gases and smaller oligomer fragments. The cracking phenomena is properly accounted for using Bethe lattice statistics. In an open system, oligomers do not decompose significantly when cooled to low temperatures. For open systems, nonreactive oligomers must be accounted for separately. In the present paper, oligomers are assumed to continue to react. The reacting oligomer assumption is thought to be reasonable since the majority of the oligomers are monomers and do not react significantly.

A detailed formulation of percolation theory based on Bethe lattices is discussed in detail by Grant et al. [3] and will not be repeated here. Differences between the application of percolation theory by Grant et al. [3] and the model discussed in the present paper are in the definitions of the population of intact bonds described by Eq. (4) and the definition of mass on a site basis. The mass fraction and molecular weight of each oligomer bin can be determined by relating the total mass and mass associated with finite oligomers on a site basis. A site is defined as the portion of the polymer that can be isolated by bonds. The total mass per site is defined as:

$$m_{tot} = M_a + \frac{M_b}{2}(1-c_o)(\sigma+1) \tag{5}$$

where M_a is the molecular weight of the site or mer, $M_b/2$ is half the molecular weight of the bridges connecting the mers, 1-c_o represents the fraction of bonds which are labile, and $\sigma + 1$ is the coordination number.

The mass of gas released can also be expressed on a site basis as

$$m_g = \left(\frac{M_b}{2}\right)(g_1+g_2)(\sigma+1) + \left(\frac{2M_b - M_{g3}}{2}\right)(g_4+g_5)\overset{(\sigma+1)}{\vee} + \left(\frac{M_{g3}}{2}\right)(g_3)(\sigma+1) \tag{6}$$

[illegible] → where M_b is the molecular weight of g_1 and g_2, $2\,M_b$ - M_{g3} is the molecular weight of g_4 and g_5, and M_{g3} is the molecular weight of $g3$. These molecular weights are divided by two to normalize the gas populations to the total mass per site given in Eq. (5) by noting

$$g_1 + g_2 + g_3 + 2g_4 + 2g_5 \rightarrow (1-c_o) \qquad \text{as} \qquad \text{time} \rightarrow \infty \tag{7}$$

The mass of a finite oligomer expressed on a site basis, m_n, can be determined from the mass of a finite oligomer, M_n, multiplied by the n-site oligomer population on a site basis, Q_n:

$$m_n = M_n Q_n \tag{8}$$

$$\text{where,} \quad M_n = nM_a + (n-1)M_b\left(\frac{\mathcal{L}}{p}\right) + (n-1)(2M_b - M_{g3})\left(\frac{\mathrm{L}}{p}\right) + \frac{M_b}{2}\left[\frac{\tau\delta}{(1-p)}\right] + \frac{(2M_b - M_{g3})}{2}\left[\frac{\tau \mathrm{d}}{(1-p)}\right] \tag{9}$$

$$Q_n = F_n/n = b_n p^{n-1}(1-p)^{n(\sigma-1)+2} \tag{10}$$

M_n is the molecular weight of the n^{th}-oligomer bin. The first term in Eq. (9) represents the number of mers in the n-mer multiplied by the mer molecular weight. The second term in Eq. (9) represents the number of bridges, n - 1, in the oligomer multiplied by the mass of the bridges of type $\mathcal{L}$. The third term in Eq. (9) represents the number of bridges in the oligomer multiplied by the mass of the bridges of type L. The last two terms in Eq. (9) represent the weight of the side-chains or "danglers" which can evolve over time. The factors $\delta/(1\text{-}p)$ and $\mathrm{d}/(1\text{-}p)$ represent the fraction of side-chains of type δ and d, respectively. The fraction of broken bridges with one side-chains being formed from each broken bridge is represented by (1-p). τ is the number of bridges that isolate an oligomer. Grant et al. [3-5] give details on calculating, Q_n, F_n and b_n.

The mass fraction g_1 through g_5 as well as the mass fraction of the polymer fragments can be determined with Eqns. (5), (6), and (8) using parameters obtained from the PUF kinetic mechanism. The overall gas, polymer fragment, and solid yields can also be determined by following the procedure outlined by Grant et al. [3-5].

VAPOR-LIQUID EQUILIBRIUM AND PARAMETER ESTIMATION

The fraction of the gaseous oligomers can be determined by using a simple vapor-liquid equilibrium relationship using a combination of Dalton's law and Raoult's law. A standard multicomponent isothermal flash calculation was used to determine the split between vapor and condensed phases following the procedure used by Fletcher et al. [5]. Details of this procedure will not be repeated.

The vapor-liquid equilibrium model requires the vapor pressure of each oligomer as a function of temperature. In the current paper, literature values [14] of vapor pressures are used for TDI (represented by g_1 and g_2) and CO_2 (g_3). The FGP vapor pressure correlation [5] is used for g_4, g_5 and all polymer fragments.

The parameters used in the PUF model are shown in Table 2. The initial bond population parameters, p_o and c_o, were estimated based on the degree of polymer curing. The coordination number and molecular weights were calculated from the three most common structural units of the foam. The Arrhenius parameters were obtained by minimizing the root mean squared error between the calculated and measured mass loss for a single isothermal TGA experiment ramped at 20 C/min [15] using DAKOTA [Design Analysis Kit for OpTimizAtion, Ref. 16]. Detailed isothermal experiments at low temperatures are currently being performed at Sandia National Laboratories to isolate the decomposition kinetics of the initial polymer and formation of the secondary polymer and will be applied to further validate/improve the PUF model in the future [11].

NONISOTHERMAL TGA EXPERIMENTS

A single nonisothermal TGA experiment with the temperature increased at 20 C/min was used to determine the kinetic parameters given in Table 2. A separate nonisothermal experiment, not used to estimate the kinetic parameters, was simulated to validate the PUF model. Acceptable agreement between predicted and measured weight loss for the two nonisothermal TGA experiments with heating rates of 20 and 200 C/min are shown in Fig 6. Figure 6 also shows population parameters, the gas and oligomer mass fractions, and gas molecular weight for the 20 C/min ramped TGA experiment. Crosslinking of the two δ side-chains to form L is apparent between 15 and 20 minutes in Fig 6.B. The reversible reaction causing reattachment of one δ side-chain to form $\mathcal{L}$ is not shown to be significant in Fig 6.B. Decay of the weak bridge L is shown as the side-chain population d increases. The strong bond formation in the primary and secondary polymer are minimal. However, the formation of strong bonds may become significant at elevated pressures. Figure 6.C shows the nonlinear nature of the molecular weight evolution of the evolving gases. The peak in gas molecular weight near 18 minutes corresponds to the maximum evolution of primary side chains, δ.

SUMMARY AND CONCLUSIONS

The PolyUrethane Foam (PUF) decomposition model is comprised of three components: 1) a kinetic mechanism which describes bond breaking, 2) a lattice statistics model to describe the mass fraction of finite oligomers isolated from the macromolecule by broken bonds, and 3) a transport model to describe the evaporation of the finite oligomers with high vapor pressures into the gas-phase. The chemical structure of the foam was deduced from synthesis details, and the PUF model parameters were obtained from the most common structural unit of the foam. Kinetic parameters for the PUF model were obtained from a single nonisothermal TGA experiment. Using the chemical structure and kinetic parameters, the model predictions were compared to data for a separate nonisothermal TGA experiment at a significantly higher heating rate with reasonable agreement. Such agreement between calculated and measured foam mass loss supports the hypothesis that improved predictions of rigid polyurethane foam decomposition can be obtained by using a more fundamental description of foam pyrolysis.

The three components of the PUF model (kinetics, statistics, vapor-liquid equilibrium) should be considered a *framework* for thermal decomposition. The kinetic bond breaking scheme can be revised to accommodate experimental discovery from ongoing rigid polyurethane decomposition experiments including additional secondary reactions. The statistics model describes the evolution of the molecular weight distributions of the finite products. The statistics model can be replaced by realistic Monte Carlo methods, or perhaps a percolation model with a variable coordination number. Improved vapor-pressure correlations specific to polyurethane decomposition fragments may also improve modeling results. The transport model can be modified to account for condensed-phase diffusion including secondary reactions and crosslinking as well as gas-phase diffusion through a boundary layer. *At this time, such modifications are unwarranted without more experimental data.* Suggestions for new experiments and modeling follow:

- Material extracted from various polyurethane samples, using suitable solvents such as tetrahydrofuran, corresponds to the finite oligomers trapped in the larger macromolecules at room temperature and pressure. The amount of extracted oligomers is expected to be related to the degree of curing and defines the initial population parameters $\mathcal{L}_0$ and c_0. Furthermore, the weight fraction of oligomers extracted from thermally degraded foams with tetrahydrofuran can be used to validate proposed chemical structures, rate expressions, and lattice statistics.

- A simpler foam composed of only one structural unit could be synthesized for validation experiments [10]. The 10% most probable structural unit as shown in Fig 4 is a likely candidate for synthesis. The decomposition products from simple foams would be easier to identify for model validation.

- Boiling points from liquids derived from decomposing foam should be used to improve vapor pressure correlations for foam fragments.

- As the foam decomposes, the finite oligomers may react or crosslink with the macromolecule causing the coordination number to increase. An increasing coordination number can not be modeled with a simple *1-σ statistical model* as discussed in this paper. Experiments, designed to characterize the reacting foam, may give insight into the evolving coordination number. Advanced statistical treatments may be necessary to model crosslinking when the average coordination number is not constant.

- Condensed-phase and gas-phase diffusion of oligomers with secondary reactions may be significant at certain temperatures and pressures. The low thermal conductivity of the foam can also cause high temperature and pressure gradients. The high temperature and pressure gradients promote nucleation of small cracks which can grow in to large fissures. The macroscale deformation of the foam during decomposition should be modeled using a constitutive model such as the Reactive Elastic Plastic (REP) constitutive model developed for energetic materials [17]. Modifications may be necessary to simulate the more porous polyurethane foam.

ACKNOWLEDGEMENTS

Experimental support from K. L. Erickson, J. Kurtz, T. Y. Chu, W. Gill, A. M. Renlund, R. S. Saunders, and T. A. Ulibarri is gratefully acknowledged. The TGA data was supplied by B. F. Blackwell. M. S. Eldred helped set up the DAKOTA optimizer used to obtain the activation energies. D. K. Gartling performed the three-dimensional calculations shown in Fig 1. Modeling discussions related to the percolation theory from D. M. Grant, R. J. Pugmire, and T. H. Fletcher are also appreciated. Comments from internal reviewers at Sandia National Laboratories, K. L. Erickson, A. R. Kerstein, and A. C. Ratzel, are also deeply appreciated.

Sandia is a multiprogram laboratory operated by Sandia Corporation, a Lockheed Martin Company, for the United States Department of Energy under contract DE-AC04-94AL85000.

REFERENCES

1. Gartling, D. K, personal communication, Sandia National Laboratories (1997)
2. Solomon, P. R., Hamblen, D. G., Carangelo, R. M., Serio, M. A., Deshpande, G. V. *Energy & Fuels* 2:405-422 (1988)
3. Grant, D. M., Pugmire, R. J., Fletcher, T. H., Kerstein, A. R., *Energy & Fuels* 3:175-186 (1989)
4. Fletcher, T. H., Kerstein, A. R., Pugmire, R. J., Grant, D. M., *Energy & Fuels* 4:54-60 (1990)
5. Fletcher, T. H., Kerstein, A. R., Pugmire, R. J., Solum, M. S., Grant, D. M., *Energy & Fuels* 6:414-431 (1992)
6. Fisher, M. E., and Essam, J. W., *Journal of Mathematical Physics* 2(2):609-619 (1961)
7. Flory, P. J., *Principles of Polymer Chemistry*, Cornell University Press, Ithaca, 1953, p 347.
8. Hobbs, M. L., Radulovic, P. T., Smoot, L. D., *Prog. Energy Combust. Sci.* 19:505-586 (1993)
9. Solum, M. S., Pugmire, R. J.,Grant, D. M., *Energy & Fuels* 3:187-193 (1989)
10. Saunders, R. and Ulibarri, T., personal communication, Sandia National Laboratories (1997)
11. Erickson, K. L., personal communication, Sandia National Laboratories (1997)
12. Shampine, L. F. and Watts, H. A., "DEPAC - Design of a User Oriented Package of ODE Solvers," Sandia National Laboratories Report No. SAND-79-2374, 1979
13. Solomon, P. R., Hamblen, D. G., Serio, M., Yu, Z., Charpenay, S., *Fuel* 72(4):469-488 (1993)
14. Daubert, T. E. and Danner, R. P. *Design Institute for physical property data*, AIChE, Dept. of Chem. Eng., Penn State University (1994)
15. Blackwell, B. F., personal communication, Sandia National Laboratories (1997)
16. Eldred, M. S., "DAKOTA Manuals," Sandia National Laboratories Report, 1998, in preparation. See also http://endo.sandia.gov/9234/sd_optim_dakota.html
17. M. L., Hobbs, Baer, M. R., and Gross, R. J., *Twentieth International Pyrotechnics Seminar*, Colorado Springs, CO, 1994, 423-436

Table1. Mechanism, rate equations, and boundary conditions for the PUF model*

Rxn	Mechanism	Species	Rate Equations	Boundary Conditions
		$\mathcal{L}$	$d\mathcal{L}/dt = -k_1\mathcal{L} - k_2\mathcal{L} + k_3\delta$	$\mathcal{L}(0) = \mathcal{L}_o$
(1)	$\mathcal{L} \rightarrow c_1 + g_1$	L	$dL/dt = k_5\delta^2 - k_6L - k_7L + k_8L$	$L(0) = 0$
(2)	$\mathcal{L} \rightarrow \delta$	δ	$d\delta/dt = k_2\mathcal{L} - k_3\delta - k_4\delta - 2k_5\delta^2$	$\delta(0) = 1 - c_o - \mathcal{L}_o$
(3)	$\delta \rightarrow \mathcal{L}$	d	$dd/dt = k_7L - k_8d - k_9d$	$d(0) = 0$
(4)	$\delta \rightarrow g_2$	c_1	$dc_1/dt = k_1\mathcal{L}$	$c_1(0) = c_o$
(5)	$2\delta \rightarrow L + g_3$	c_2	$dc_2/dt = k_6L$	$c_2(0) = 0$
(6)	$L \rightarrow c_2 + g_4$	g_1	$dg_1/dt = k_1\mathcal{L}$	$g_1(0) = 0$
(7)	$L \rightarrow d$	g_2	$dg_2/dt = k_4\delta$	$g_2(0) = 0$
(8)	$d \rightarrow L$	g_3	$dg_3/dt = k_5\delta^2$	$g_3(0) = 0$
(9)	$d \rightarrow g_5$	g_4	$dg_4/dt = k_6L$	$g_4(0) = 0$
		g_5	$dg_5/dt = k_9d$	$g_5(0) = 0$

* The concentration (μ_{ij}) and stoichiometric matrices (ν_{ij}) with the reactions loaded into 9 columns ($j = 9$) and the species loaded into eleven rows ($i = 11$) are written as:

$$\mu_{ij} = \begin{array}{c|ccccccccc|}
 & r_1 & r_2 & r_3 & r_4 & r_5 & r_6 & r_7 & r_8 & r_9 \\
\mathcal{L} & 1 & 1 & 0 & 0 & 0 & 0 & 0 & 0 & 0 \\
L & 0 & 0 & 0 & 0 & 0 & 1 & 1 & 0 & 0 \\
\delta & 0 & 0 & 1 & 1 & 2 & 0 & 0 & 0 & 0 \\
d & 0 & 0 & 0 & 0 & 0 & 0 & 0 & 1 & 1 \\
c1 & 0 & 0 & 0 & 0 & 0 & 0 & 0 & 0 & 0 \\
c2 & 0 & 0 & 0 & 0 & 0 & 0 & 0 & 0 & 0 \\
g1 & 0 & 0 & 0 & 0 & 0 & 0 & 0 & 0 & 0 \\
g2 & 0 & 0 & 0 & 0 & 0 & 0 & 0 & 0 & 0 \\
g3 & 0 & 0 & 0 & 0 & 0 & 0 & 0 & 0 & 0 \\
g4 & 0 & 0 & 0 & 0 & 0 & 0 & 0 & 0 & 0 \\
g5 & 0 & 0 & 0 & 0 & 0 & 0 & 0 & 0 & 0
\end{array}
\qquad
\nu_{ij} = \begin{array}{c|ccccccccc|}
 & r_1 & r_2 & r_3 & r_4 & r_5 & r_6 & r_7 & r_8 & r_9 \\
d\mathcal{L}/dt & -1 & -1 & +1 & 0 & 0 & 0 & 0 & 0 & 0 \\
dL/dt & 0 & 0 & 0 & 0 & +1 & -1 & -1 & +1 & 0 \\
d\delta/dt & 0 & +1 & -1 & -1 & -2 & 0 & 0 & 0 & 0 \\
dd/dt & 0 & 0 & 0 & 0 & 0 & 0 & +1 & -1 & -1 \\
dc1/dt & +1 & 0 & 0 & 0 & 0 & 0 & 0 & 0 & 0 \\
dc2/dt & 0 & 0 & 0 & 0 & 0 & +1 & 0 & 0 & 0 \\
dg1/dt & +1 & 0 & 0 & 0 & 0 & 0 & 0 & 0 & 0 \\
dg2/dt & 0 & 0 & 0 & +1 & 0 & 0 & 0 & 0 & 0 \\
dg3/dt & 0 & 0 & 0 & 0 & +1 & 0 & 0 & 0 & 0 \\
dg4/dt & 0 & 0 & 0 & 0 & 0 & +1 & 0 & 0 & 0 \\
dg5/dt & 0 & 0 & 0 & 0 & 0 & 0 & 0 & 0 & +1
\end{array}$$

Table 2. Parameters used in the PUF model*

Parameter	Description	Values
P_o	Initial population of weak bonds	0.85
c_o	Initial population of strong bonds	0.10
$\sigma + 1$	Coordination number	2.8
M_a	Molecular weight of mer without side chains	125 kg/kmol
M_b	Molecular weight of bridge	161 kg/kmol
M_{g3}	Molecular weight of g_3 assumed to be CO_2	44 kg/kmol
E_1/R	Activation energy of reaction 1 divided by gas constant	30100 K
E_2/R	Activation energy of reaction 2 divided by gas constant	25400 K
E_3/R	Activation energy of reaction 3 divided by gas constant	25600 K
E_4/R	Activation energy of reaction 4 divided by gas constant	26400 K
E_5/R	Activation energy of reaction 5 divided by gas constant	26200 K
E_6/R	Activation energy of reaction 6 divided by gas constant	32600 K
E_7/R	Activation energy of reaction 7 divided by gas constant	29900 K
E_8/R	Activation energy of reaction 8 divided by gas constant	30200 K
E_9/R	Activation energy of reaction 9 divided by gas constant	32200 K

* All frequency factors, *A*, were assumed to be equal to 3.0×10^{15} s^{-1} and the barometric pressure in Albuquerque was taken to be 12 psia (82737 Pa).

List of Figures

Fig 1. Example calculation of inert components encapsulated in rigid polyurethane foam exposed to a constant flux on the entire exposed surface. The initial temperature of the block was assumed to be 100 C with the bottom plate held at a constant temperature. Initially, 23,500 elements were used in the system with elements dynamically removed when element temperature exceeded 150 C. Figure used with permission from Gartling [1].

Fig 2. Synthesis of a simple polyurethane foam showing a conceptualized structure of foam in a real lattice. $\sigma + 1$ is the coordination number of each cluster

Fig 3. Real polyurethane lattice described by a pseudo Bethe lattice. The thermal decomposition of the polyurethane is described by bond breaking which isolates finite fragments (shown as 2-D circles) from the infinite lattice network (shown as 3-D spheres).

Fig 4. Most common chemical structural units and hypothetical chemical structure of rigid polyurethane foam. The graphic symbols are composed of ingredients used to make the specific foam.

Fig 5. Kinetic mechanism for decomposition of rigid polyurethane foam. Initial decomposition of the polyurethane foam is depicted using the most common structural unit of the foam.

Fig 6. A) Comparison of predicted (solid line) and measured (symbols) solid mass fractions from two different nonisothermal TGA experiments. B) Predicted population parameters for the 20 C/min TGA experiment. C) Predicted average volatile molecular weight and various oligomer mass percents for the 20 C/min TGA experiment.

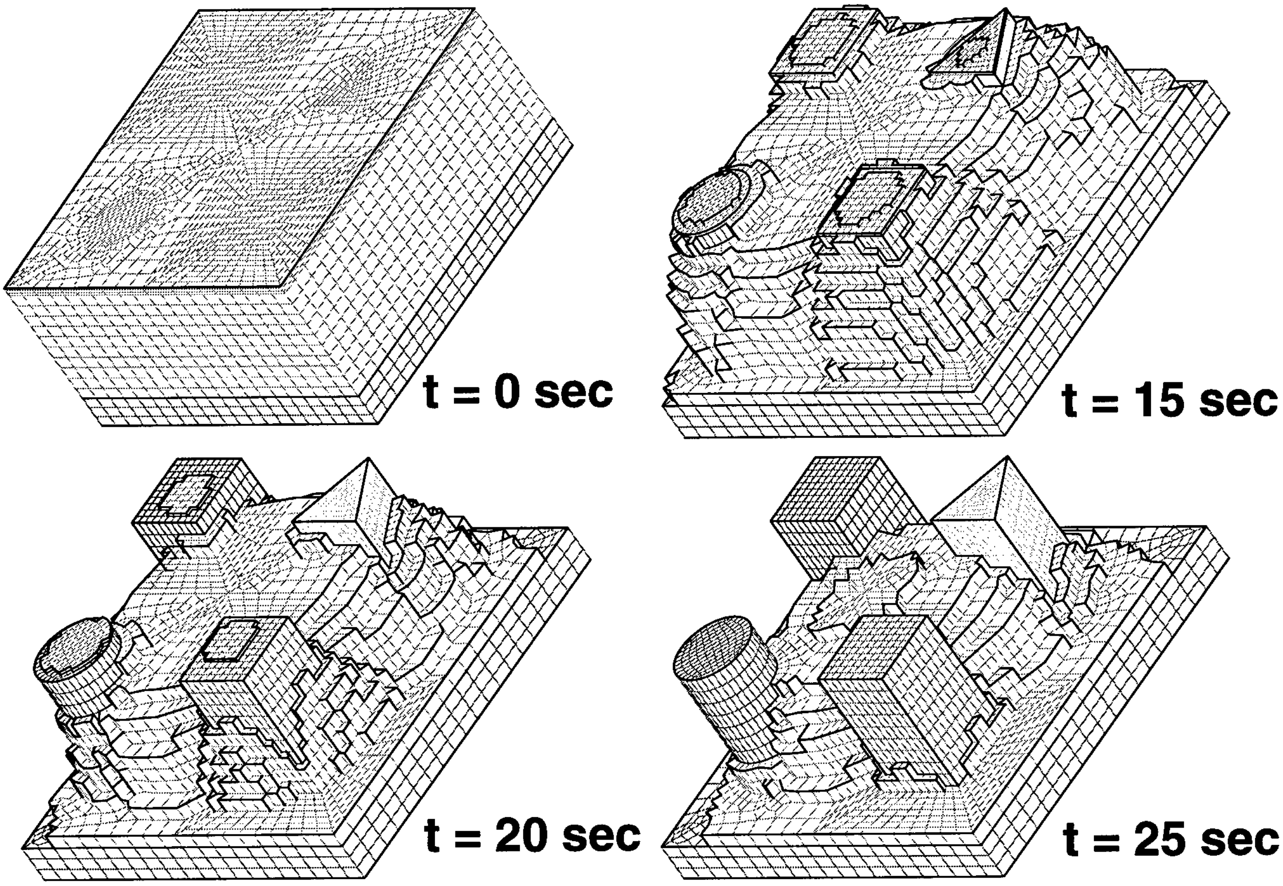
t = 0 sec
t = 15 sec
t = 20 sec
t = 25 sec

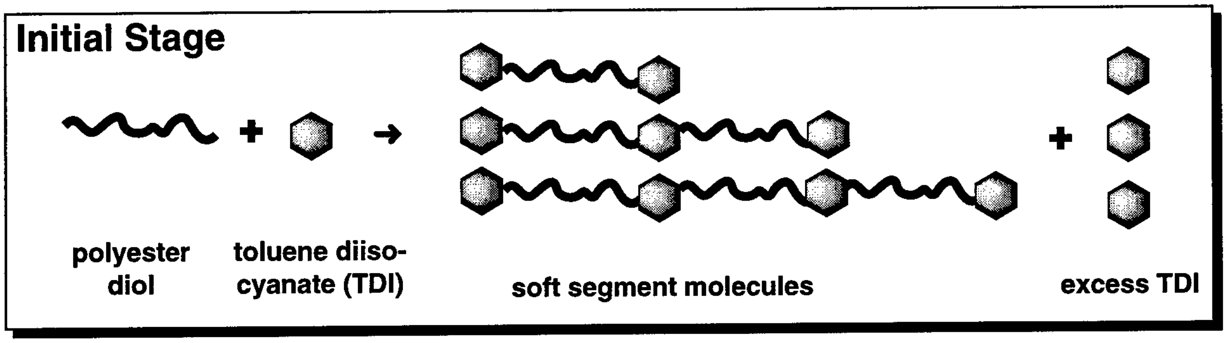
Initial Stage
+
→
+
polyester diol
toluene diisocyanate (TDI)
soft segment molecules
excess TDI

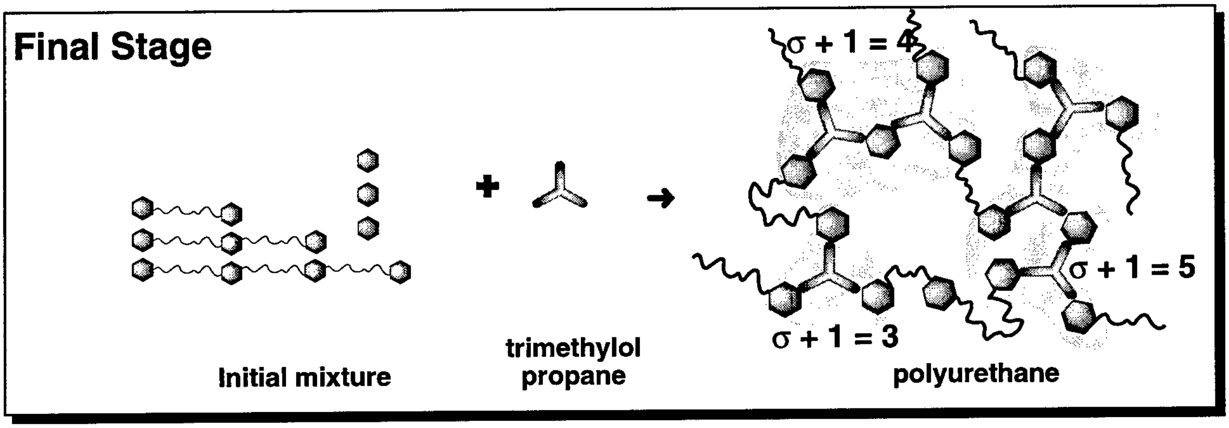
Final Stage
+
→
σ + 1 = 4
σ + 1 = 5
σ + 1 = 3
Initial mixture
trimethylol propane
polyurethane

Decomposition Chemistry Described by Bond Breaking

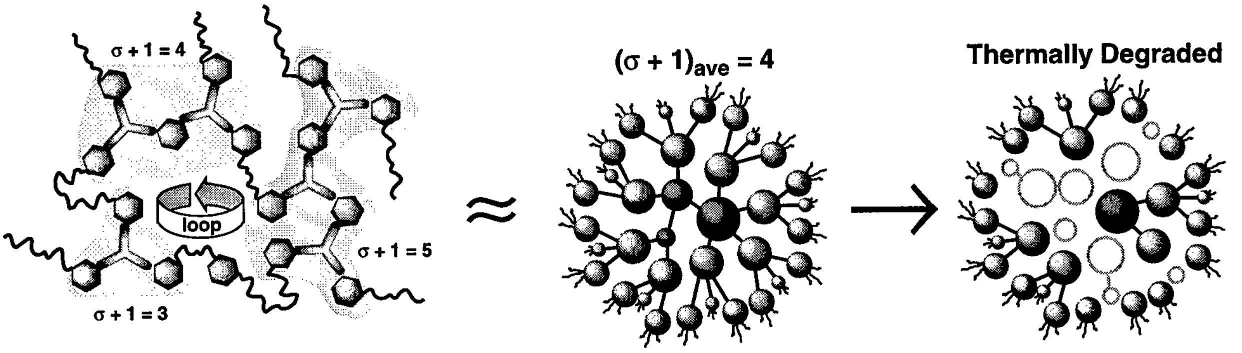

Real polyurethane lattice
(Clusters are shaded)

Pseudo-lattice with no loop-backs
(Clusters represented as spheres)

Finite fragments (circles)
Infinite network (spheres)

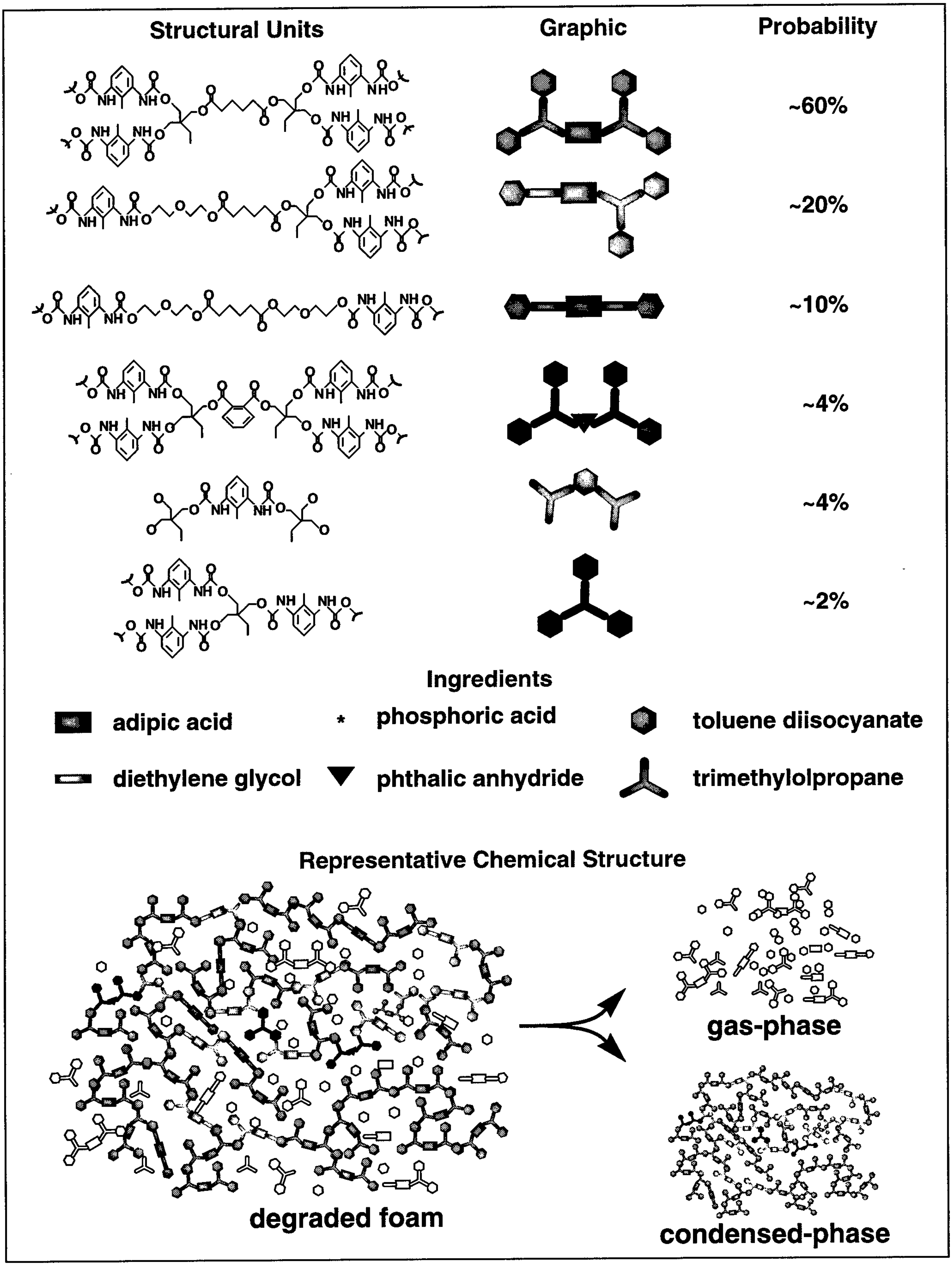
Structural Units
Graphic
Probability
~60%
~20%
~10%
~4%
~4%
~2%
Ingredients
adipic acid
phosphoric acid
toluene diisocyanate
diethylene glycol
phthalic anhydride
trimethylolpropane
Representative Chemical Structure
degraded foam
gas-phase
condensed-phase

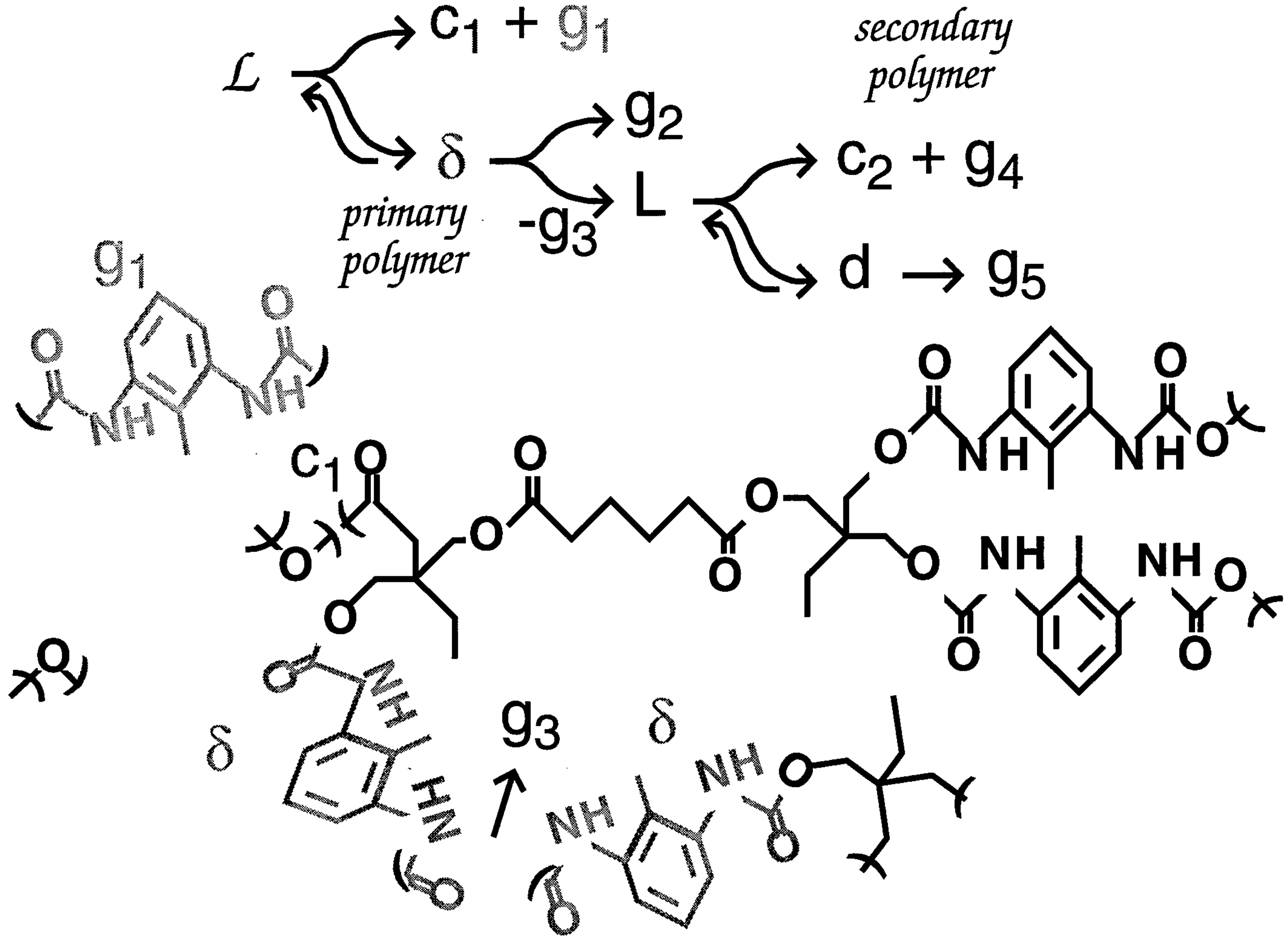
ℒ
c1 + g1
δ
g2
-g3
L
c2 + g4
d → g5
primary polymer
secondary polymer
g1
c1
δ
g3
δ
NH
O

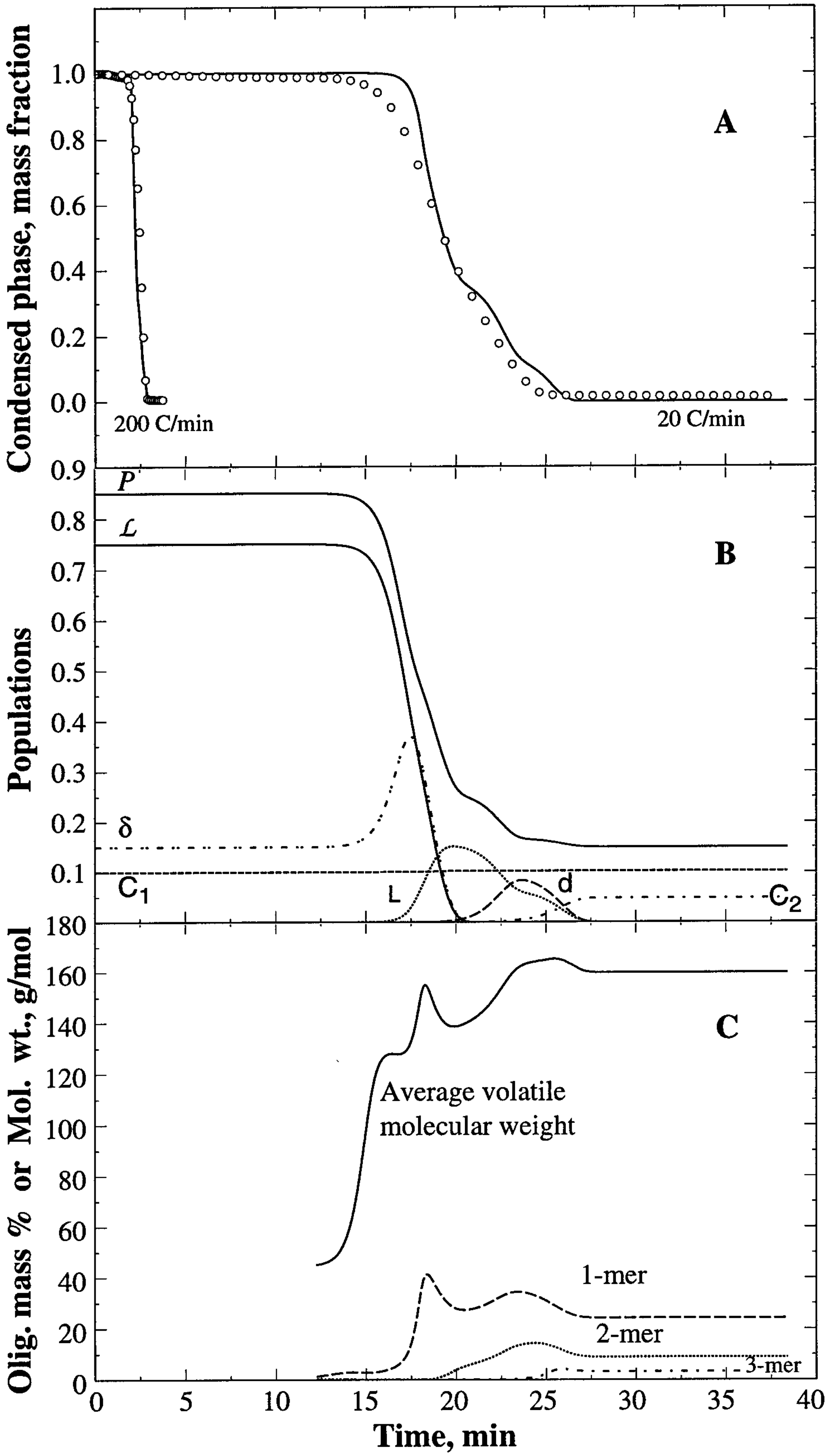
Condensed phase, mass fraction
1.0
0.8
0.6
0.4
0.2
0.0
A
200 C/min
20 C/min
Populations
0.9
0.8
0.7
0.6
0.5
0.4
0.3
0.2
0.1
P
ℒ
B
δ
C1
L
d
C2
Olig. mass % or Mol. wt., g/mol
180
160
140
120
100
80
60
40
20
0
C
Average volatile
molecular weight
1-mer
2-mer
3-mer
0
5
10
15
20
25
30
35
40
Time, min

Report Number (14) SAND-98-0065C
CONF-980804--

Publ. Date (11) 199801
Sponsor Code (18) DOE/DP, XF
UC Category (19) UC-700, DOE/ER